Reconfigurable optical routers based on Coupled Resonator Induced Transparency resonances

M. Mancinelli,[1,*] P. Bettotti,[1] J.M. Fedeli,[2] and L. Pavesi[1]

1. Nanoscience Laboratory, Department of Physics, University of Trento, Via Sommarive 14, I-38123 Povo (Trento), Italy

2. CEA, Lèti, Minatec campus 17 Rue des Martyrs, 38054 Grenoble cedex 9, France

[*]mancinelli@science.unitn.it

Abstract: The interferometric coupling of pairs of resonators in a resonator sequence generates coupled ring induced transparency (CRIT) resonances. These have quality factors an order of magnitude greater than those of single resonators. We show that it is possible to engineer CRIT resonances in tapered SCISSOR (Side Coupled Integrated Space Sequence of Resonator) to realize fast and efficient reconfigurable optical switches and routers handling several channels while keeping single channel addressing capabilities. Tapered SCISSORs are fabricated in silicon-on-insulator technology. Furthermore, tapered SCISSORs show multiple-channel switching behavior that can be exploited in DWDM applications.

OCIS codes: (230.4555) Coupled resonators; (250.5300) Photonic integrated circuits.

References and links

1. M. Lipson, "Guiding, modulating, and emitting light on silicon - Challenges and opportunities," J. Lightwave Technol. **23**(12), 4222–4238 (2005).
2. Y. Vlasov, W. M. J. Green, and F. Xia, "High-Through put silicon nanophotonic wavelength-insensitive switch for on-chip optical networks," Nat. Photonics **2**(4), 242–246 (2008).
3. A. Shacham, K. Bergman, and L. P. Carloni, "Photonic networks-on-chip for future generations of chip multiprocessors," IEEE Trans. Comput. **57**(9), 1246–1260 (2008).
4. X. Z. Zheng, F. Y. Liu, J. Lexau, D. Patil, G. L. Li, Y. Luo, H. D. Thacker, I. Shubin, J. Yao, K. Raj, R. Ho, J. E. Cunningham, and A. V. Krishnamoorthy, "Ultralow power 80 gb/s arrayed cmos silicon photonic transceivers for wdm optical links," J. Lightwave Technol. **30**(4), 641–650 (2012).
5. S. Feng, T. Lei, H. Chen, H. Cai, X. Luo, and A. W. Poon, "Silicon photonics: from a microresonator perspective," Laser Photon. Rev. **6**(2), 145–177 (2012).
6. W. Bogaerts, P. De Heyn, T. Van Vaerenbergh, K. De Vos, S. Kumar Selvaraja, T. Claes, P. Dumon, P. Bienstman, D. Van Thourhout, and R. Baets, "Silicon microring resonators," Laser Photon. Rev. **6**(1), 47–73 (2012).
7. J. E. Heebner, R. W. Boyd, and Q. H. Park, "SCISSOR solitons and other novel propagation effects in microresonator-modified waveguides," J. Opt. Soc. Am. B **19**(4), 722–731 (2002).
8. S.-Y. Cho and R. Soref, "Apodized SCISSORs for filtering and switching," Opt. Express **16**(23), 19078–19090 (2008).
9. Q. F. Xu, S. Sandhu, M. L. Povinelli, J. Shakya, S. H. Fan, and M. Lipson, "Experimental realization of an on-chip all-optical analogue to electromagnetically induced transparency," Phys. Rev. Lett. **96**(12), 123901 (2006).
10. B. E. Little, J. P. Laine, and S. T. Chu, "Surface-roughness-induced contradirectional coupling in ring and disk resonators," Opt. Lett. **22**(1), 4–6 (1997).
11. J. E. Heebner, P. Chak, S. Pereira, J. E. Sipe, and R. W. Boyd, "Distributed and localized feedback in microresonator sequences for linear and nonlinear optics," J. Opt. Soc. Am. B **21**(10), 1818–1832 (2004).
12. M. Mancinelli, R. Guider, P. Bettotti, M. Masi, M. R. Vanacharla, and L. Pavesi, "Coupled-resonator-induced-transparency concept for wavelength routing applications," Opt. Express **19**(13), 12227–12240 (2011).
13. M. Mancinelli, R. Guider, M. Masi, P. Bettotti, M. R. Vanacharla, J.-M. Fedeli, and L. Pavesi, "Optical characterization of a SCISSOR device," Opt. Express **19**(14), 13664–13674 (2011).
14. S. F. Mingaleev, A. E. Miroshnichenko, and Y. S. Kivshar, "Coupled-resonator-induced reflection in photonic-crystal waveguide structures," Opt. Express **16**(15), 11647–11659 (2008).
15. Y.-F. Xiao, X.-B. Zou, W. Jiang, Y.-L. Chen, and G.-C. Guo, "Analog to multiple electromagnetically induced transparency in all-optical drop-filter systems," Phys. Rev. A **75**(6), 063833 (2007).
16. X. Yang, M. Yu, D.-L. Kwong, and C. W. Wong, "All-optical analog to electromagnetically induced transparency in multiple coupled photonic crystal cavities," Phys. Rev. Lett. **102**(17), 173902 (2009).

#174511 - $15.00 USD Received 16 Aug 2012; revised 27 Sep 2012; accepted 27 Sep 2012; published 3 Oct 2012

17. X. Wang, J. A. Martinez, M. S. Nawrocka, and R. R. Panepucci, "Compact thermally tunable silicon wavelength switch: modeling and characterization," IEEE Photon. Technol. Lett. **20**(11), 936–938 (2008).
18. P. Dong, W. Qian, H. Liang, R. Shafiiha, D. Feng, G. Li, J. E. Cunningham, A. V. Krishnamoorthy, and M. Asghari, "Thermally tunable silicon racetrack resonators with ultralow tuning power," Opt. Express **18**(19), 20298–20304 (2010).
19. F. Y. Gardes, D. J. Thomson, N. G. Emerson, and G. T. Reed, "40 Gb/s silicon photonics modulator for TE and TM polarisations," Opt. Express **19**(12), 11804–11814 (2011).
20. E. J. Klein, P. Urban, G. Sengo, L. T. H. Hilderink, M. Hoekman, R. Pellens, P. van Dijk, and A. Driessen, "Densely integrated microring resonator based photonic devices for use in access networks," Opt. Express **15**(16), 10346–10355 (2007).
21. H. Shen, M. H. Khan, L. Fan, L. Zhao, Y. Xuan, J. Ouyang, L. T. Varghese, and M. Qi, "Eight-channel reconfigurable microring filters with tunable frequency, extinction ratio and bandwidth," Opt. Express **18**(17), 18067–18076 (2010).
22. M. S. Dahlem, C. W. Holzwarth, A. Khilo, F. X. Kärtner, H. I. Smith, and E. P. Ippen, "Reconfigurable multi-channel second-order silicon microring-resonator filterbanks for on-chip WDM systems," Opt. Express **19**(1), 306–316 (2011).

1. Introduction

Silicon photonics is the technology to develop next generation opto-electronic and all-optical integrated devices [1]. It allows increasing the integration level of photonic circuits at the levels required by complex network on chip or signal optical processing systems for chip-to-chip and on-chip applications [2,3]. A key element for any of these applications is the switching port. The most successful switching ports are based on single microring resonators where the ring resonance rules the behavior of the port. Single switches and complex resonator fabrics have shown very high performance, very large bandwidths as well as extremely low power consumption [4]. Still these schemes cannot be readily integrated onto on chip DWDM (dense wavelength division multiplexing, channel spacing 100 GHz) or UDWDM (ultra dense wavelength division multiplexing, channel spacing 25 GHz) applications because of the very strict fabrication tolerances they require, of the necessary great control over the (low) bus waveguide to resonator coupling coefficient, and both tuning and trimming issues of switching methods based on resonance shifts [5,6].

In this paper, we show that the optical feedback provided by a sequence of coupled resonators in a tapered SCISSOR (Side Coupled Integrated Spaced Sequence of Resonators [7–9]) overcomes the limitations of single ring resonators, and can be used to engineer devices robust against fabrication defects, fully supporting DWDM channel spacing and easily extendible to UDWDM. Tapered SCISSOR operates in an overcoupled regime, thus reducing insertion losses and avoiding mode splitting due contradirectional propagating modes, still preserving high Q-factor resonances [10]. Furthermore, we experimentally demonstrate that tapered SCISSOR is capable to address single channel I/O operation and it shows a fast, efficient and truly on/off switching mechanism.

1.2. Principle of operation of the tapered SCISSOR

When a sequence of resonators, e. g. racetrack resonators, is aligned in a double sided SCISSOR, the important geometrical parameters are the single resonator radius R and the resonator spacing L (Fig. 1). They regulate the different resonant mechanisms of SCISSOR:

- the single resonator resonance: $m \lambda_r = 2\pi R n_{eB} + 2 C n_{eS}$
- the Bragg-like resonance due to the periodic repetition of the resonators: $\lambda \lambda_B = 2 (L + C) n_{eS}$

where m and λ are the resonance orders, λ_r and λ_B the resonance wavelengths, C the straight waveguide section length in the racetrack, n_{eS} the effective index of the waveguide, and n_{eB} the effective index in the bend part of the racetrack resonator. These two resonances are visible in the Through port transmission spectrum of a SCISSOR as two separated stop-bands (Fig. 1(b), black line). When a tapering is made on the racetrack radii –i.e., each one is increased by ΔR – these stop-bands widen. In addition, they overlap when $m \lambda_r = \lambda \lambda_B$, that is when $\pi R n_{eB} = L n_{eS}$. Interestingly, in a tapered SCISSOR a further resonance appears within

#174511 - $15.00 USD Received 16 Aug 2012; revised 27 Sep 2012; accepted 27 Sep 2012; published 3 Oct 2012

the stop band when L has a value which is the mean of two adjacent racetrack radii (Fig. 1(c)). This resonance, named Coupled Resonator Induced Transparency (CRIT), arises from the coupling of slightly detuned resonances, mediated by the optical feedback (Bragg condition) provided by the bus waveguides [9,11]. Indeed it is very important that the Bragg and resonator resonances overlap as well as that the two racetracks have slightly different radii in order to observe CRIT resonances. In the inset of Fig. 1(c), it is shown that the CRIT resonance vanishes when the difference between the radii goes to zero. The resonator pair which yields the CRIT resonance is fixed by the length of L. Since CRIT arises from coupling between different cavities, in a tapered SCISSOR formed by N resonators there might be more than one CRIT resonance. Alternative designs to yield CRIT resonances in a tapered SCISSOR are discussed in [12].

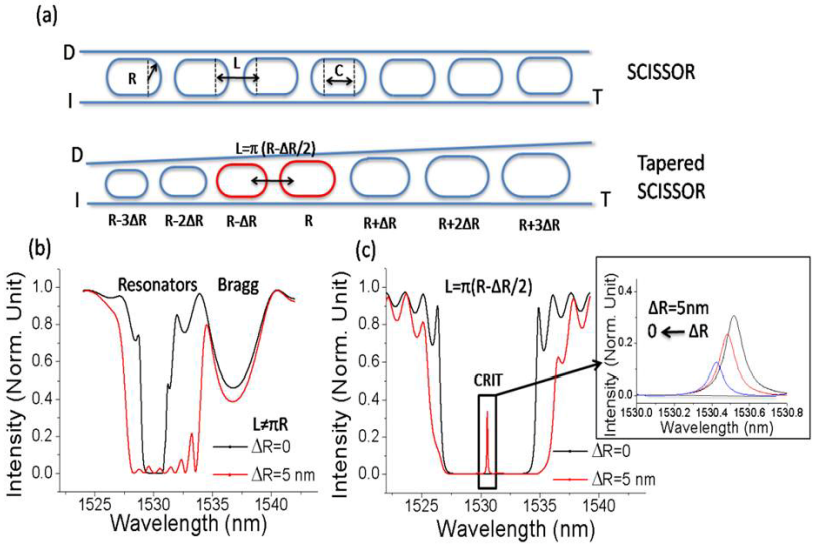

Fig. 1. (a)A double sided SCISSOR is composed by a chain of N resonators coupled by two side waveguides. The input port is label I, while the two output ports are labeled T, for the Through port, and D for the drop port. In our design, we used racetrack resonators instead of ring resonators because they provide a larger coupling for TE polarized light. Each racetrack resonator is characterized by a radius R and a coupling section C. While L defines the cavity separation. The coupling coefficient between the waveguide and the racetracks is set by the length of the coupling section (C) and by the gap between waveguides and resonator. In a tapered SCISSOR each racetrack resonator has radius which differs by ΔR from its neighbor.(b) Simulations of the Through port transmission in a SCISSOR (black line) and in a tapered SCISSOR (red line) for nondegenerate resonator and Bragg resonances. Simulation parameters: R = 3.250 μm, C = 7 μm, L = 5.105 μm, gap = 200 nm. (c) Simulations of the Through port transmission in a SCISSOR (black line) and for a tapered SCISSOR (red line) when the resonator and Bragg resonances overlap. The inset shows the dependence of the CRIT resonance on ΔR. Simulation parameters: R = 3.250 μm, C = 7 μm, L = 10.210 μm (black line) 10.200 μm (red line), gap = 160 nm.

2. Device fabrication and characterization set-up

Tapered SCISSORs were fabricated on a 200 mm SOI (silicon on insulator) wafer using 193 nm deep UV lithography. The SOI wafer consists of 220 nm thick silicon layer laid on top of 2 μm thick buried oxide. After patterning and etching, a 700 nm thick silica layer is deposited to form buried channel waveguides. Then after deposition of a 100 nm thick Ti/TiN layer, the heaters are formed by RIE etching. The silicon waveguide for both racetracks and waveguides are 500 nm wide and 220 nm thick. The actual tapered SCISSOR is composed by 7 racetrack resonators with R = 3.250 μm, L = 10.200 μm, ΔR = 5nm, C = 7μm and a racetrack-waveguide gap of 160 nm. All the parameters are optimized to work with TE polarized light.

#174511 - $15.00 USD Received 16 Aug 2012; revised 27 Sep 2012; accepted 27 Sep 2012; published 3 Oct 2012

To simulate the tapered SCISSOR, we used a standard transfer matrix method (TMM) [13]. All the lengths have been rounded to 5 nm, to match the lithography grid. The effect of the heater is taken into account using an experimental calibration curve (obtained on an isolated ring) that relates the refractive index variation in the waveguide to the electrical power used in the heater.

To characterize the tapered SCISSOR we used a tunable laser (tuning range 1260 – 1630 nm). The laser is interfaced to a single-mode fiber coupled to a polarizer and, then, to a tapered fiber tip to input the signal into the device. In this way the insertion losses are kept low (< 10 dB) in the entire bandwidth of input signal. The light at the output end of the waveguide is collected by an objective (x25) matched to an optical zoom (x7). To normalize the output power in the transmission all measurements were corrected by the transmission of the reference waveguide. A beam splitter at the output end splits the signal to an IR CCD camera for imaging the optical mode and to a detector (Ge) to measure the signal intensity. For the time resolved experiments, a Ti:Sa pulsed laser (pulse wavelength 800 nm, pulse duration 6 ps, pulse repetition rate 1 kHz) was focused on a single racetrack resonator surface with a spot diameter of about 10 μm. The mean power was 4 mW. We detect the modulated signal with a fast avalanche photodetector (time constant: 50 ps) connected to a 6 GHz oscilloscope.

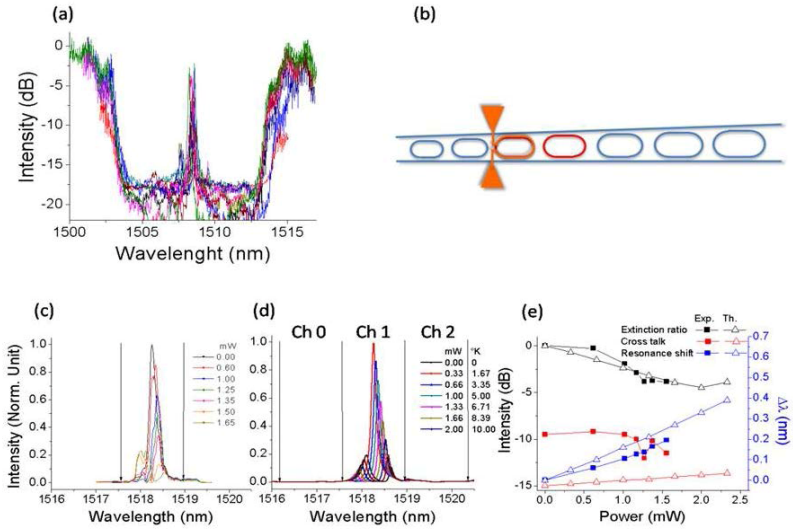

Fig. 2. (a) Through port transmission spectra of twenty equal tapered SCISSORs chosen randomly on a 200 mm wafer. (b) Sketch of a tapered SCISSOR with integrated a metal resistor to heat locally racetrack #3, counting from the left, which is paired to racetrack #4 (in red). (c) Experimental and (d) simulated Through port transmission spectra for various injected power in the heater. The vertical arrows define the transmission channels labeled CH0, CH1 and CH2. (e) Extinction ratio of CH1 (black squares), cross talk of CH1 to CH2 (red squares) and shift of the CRIT resonance in CH1 (blue squares) as a function of the heater power (open triangle symbols refer to simulation values).

3. Tapered SCISSOR measurements

Figure 2(a) reports data of nominally identical tapered SCISSOR taken randomly on various wafer dies. In all the spectra, the CRIT resonance is observed due to the central resonator pairing (shown in red in Fig. 2(b)). Despite the small racetrack average radius (3.250 μm), the CRIT resonances exhibit a Q-factor of over 11000, much greater than those of the single resonators. The high Q-factor values of the CRIT resonance are a consequence of the coupling between multiple cavities – similarly to what happens for the electromagnetic induced transparency in the atomic case - as it was recently pointed out in [14–16]. Furthermore, once

#174511 - $15.00 USD Received 16 Aug 2012; revised 27 Sep 2012; accepted 27 Sep 2012; published 3 Oct 2012

we align the low wavelength edge (maximum shift of ~5 nm) of the Through transmission stop band of the various tapered SCISSOR to take into account the typical variation of the silicon thickness in a SOI wafer, all the CRIT resonances are at the same wavelength (standard deviation in the resonance position 0.13 nm). This means that the design is robust with respect to lithography errors, while the precision on the silicon thickness in the wafer causes the randomness.

By locally change the effective mode index of a single racetrack in the pair we control the occurrence of the CRIT resonance. Figure 2(b) shows the device structure where a thermal heater is applied to racetrack #3. Due to the thermo-optic effect, the effective index of the resonant mode of racetrack #3 increases and, therefore, the ΔR between the active racetrack pair is compensated making the optical path of the two resonant modes in the two racetracks equals. Thus, the CRIT resonance is suppressed (Figs. 2(c) and 2(d)). The new functionality introduced by the CRIT is the fact that the resonance is switched off without a significant wavelength shift. This is a peculiar characteristic of CRIT compared to other resonator based switching elements. Typically, with 2 mW of electrical power injected in the heater, we fully switch off the resonance with a variation in the refractive index of $\Delta n = 4x10^{-4}$ (see Fig. 2(e)).

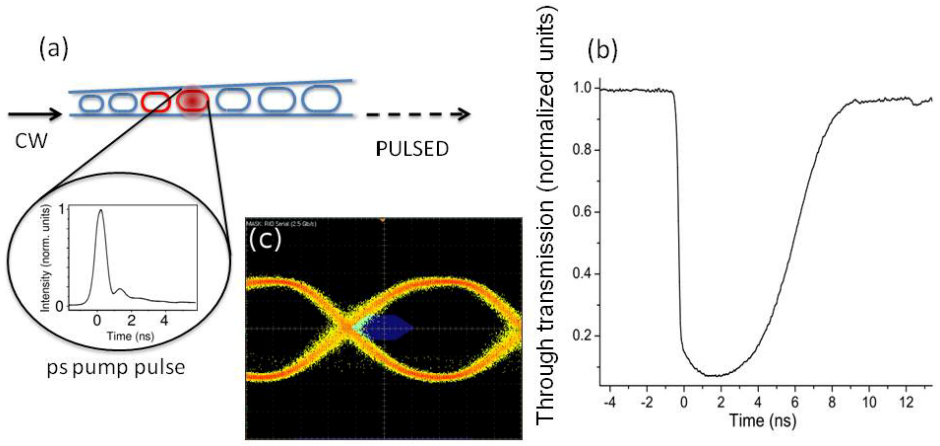

Fig. 3. (a) Sketch of the all-optical switching experiment:one of the resonator involved in the CRIT is excited with a Ti:Sa ps pulsed laser while a CW signal resonant with the CRIT resonance is input in the tapered SCISSOR.The Through port transmission is measured.(b) Normalized Through port transmission as a function of time. (c) The eye diagram shows the transmission of a 3 Gbps random sequence through a CRIT resonance.

Let us define transmission channel the spectral region centered on a CRIT resonance and with a width equal to the separation between two nearby CRIT resonances (spectral width 1.4nm ~180 GHz). This channel is named CH1, while the adjacent channels CH0 and CH2, being CH2 at longer wavelengths. Figures 2(c) and 2(d) show that the CRIT resonance attenuates within its transmission channel as the heater power increases. The maximum transmission intensity at the CRIT wavelength decreases by more than −10 dB. If we define extinction ratio as the ratio of the integrated transmitted signals in the on and off states, an extinction ratio of −4 dB is observed due to the appearance of side peaks. On the other hand, the cross talk, defined as the ratio between the transmission integrated on CH2 to that of CH1, shows a weak dependence on the heater power and starts from a value of −15 dB to reach a value of −13 dB at the maximum extinction ratio (data shown in Fig. 2(e)). This is the worst case scenario because the red shift induced by the thermal tuning would move the CRIT resonance towards CH2.

Tapered SCISSOR allows addressing the single resonator without significant changes in the collective behavior of the resonator sequence. The thermal tuning of a single resonator does not affect the spectral position of the SCISSOR stop-band (the blue edge shifts only by

#174511 - $15.00 USD Received 16 Aug 2012; revised 27 Sep 2012; accepted 27 Sep 2012; published 3 Oct 2012

0.1 nm, while the red edge does not shift). Furthermore, even using a non optimized heater, the power required to switch a CRIT resonance is of the order of 1.5 mW. This is a switching efficiency two to three times higher than those recently reported for single resonator devices of comparable size [17,18].

The dynamic properties of the tapered SCISSOR, i.e. the speed at which we can switch the single CRIT resonance, have been studied by using a Ti:Sa pulsed laser, focused on a single racetrack. In this way, free carriers are locally generated and the effective refractive index of the optical mode can be changed (Fig. 3(a)). Since free carrier refraction induces a blue shift of the resonance, we perturbed racetracks #4 in order to study the dynamical effects on CH1.The transmission of a CW signal beam, resonant with CH1, is monitored as a function of time (Fig. 3(b)).

As expected, the switching rate is limited by the recovery time due to free carrier recombinations. Indeed,fall off times as short as 130 ps (limited by the oscilloscope bandwidth) and rising times of 1.5 ns were measured. A modulation depth of 10 dB was also measured which is compatible with the results of the static experiments. Note that these performances are suitable for improvement if p-i-n structure like the one used in interferometric modulators are integrated in the tapered SCISSOR [19]. Since the CRIT narrow linewidth could limit its application to channel high frequency data, we test the dynamic capability of the device by sending a 3 Gbps signal tuned at the CRIT resonance. Figure 3(c) reports the open eye diagram (the bit rate was limited by our experimental set-up). The theoretical limit posed by the linewidth of the CRIT resonance is 60 Gbps [12].

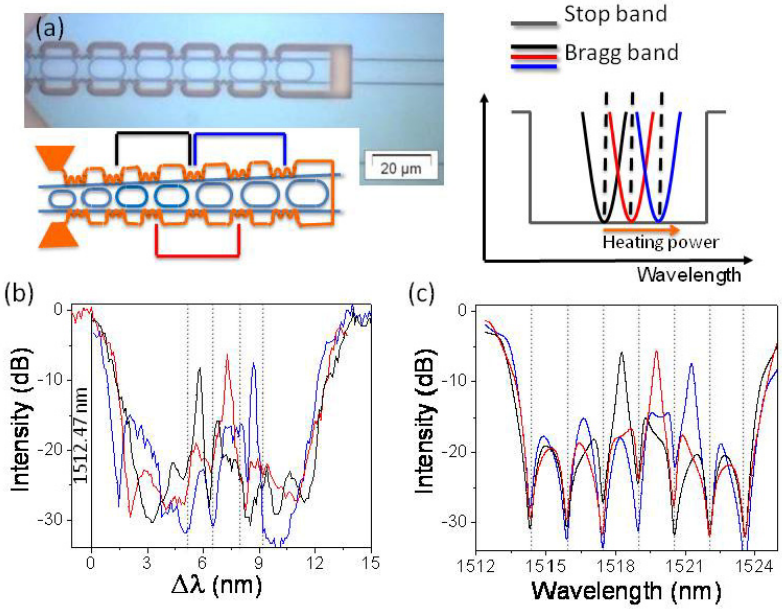

Fig. 4. (a) Optical image (top left) and sketch(bottom left) of the tapered SCISSOR. In the optical image, orange refers to the metal lines, dark blue to the waveguide and pale blue to the silicon wafer. In the sketch the difference in radius among the racetracks is greatly enhanced. Theblue, red and black lines indicate the resonators involved in the formation of the CRIT resonances when the heater heats the waveguides. A sketch of the operating principle is shown on the right. (b) Through port transmission for different heater powers: 0 mW (black), 27 mW (red), 52mW (blue).Dashed lines delimit the widths of the transmission channels. Robustness of the CRIT resonance position versus thermal tuning is clearly demonstrated in Fig. 2. (c) Simulated Through port transmission for the tapered SCISSOR. The different lines correspond to L = 10.200µm (black line), 10.220µm (red line) and 10.235µm (blue line).

An additional tuning possibility is offered by the tapered SCISSOR geometry. In fact, the CRIT resonance is also affected by the collective properties of the SCISSOR sequence, i. e.

#174511 - $15.00 USD Received 16 Aug 2012; revised 27 Sep 2012; accepted 27 Sep 2012; published 3 Oct 2012

by the Bragg condition. Figure 4(a) shows a tapered SCISSOR where serpentine heaters are overlapped with the side waveguides. In this way, the effective index of the waveguides is modified and, therefore, the Bragg stop-band is shifted within the wider resonator stop-band (Fig. 4(a)). Shifting the Bragg resonance selects a different racetrack pair for the CRIT resonance. This is confirmed in Figs. 4(b) and 4(c) where, by increasing the injected power in the heater, we switch different channels. It has to be noted that because of the proximity of the thermal heater to the cavities, the resonators are heated too. This causes a rigid shift of the entire resonator stop band. Therefore, to clearly underline the effect of heating on the single channels we rigidly shift the spectra and assume the low energy resonator band edge as the zero of the wavelength axis. Normalized spectra are then reported as a function of the wavelength shift from this common point. It is clear that the main spectral features are largely unaffected by the resonator heating. This limitation can be easily solved by using a larger separation between the resonators or a better heater design. It is therefore possible to open and close multiple independent transmission channels by using a single tapered SCISSOR where each channel is individually addressed. This is a second peculiar functionality of the proposed device that cannot be achieved using single resonator add/drop filter.

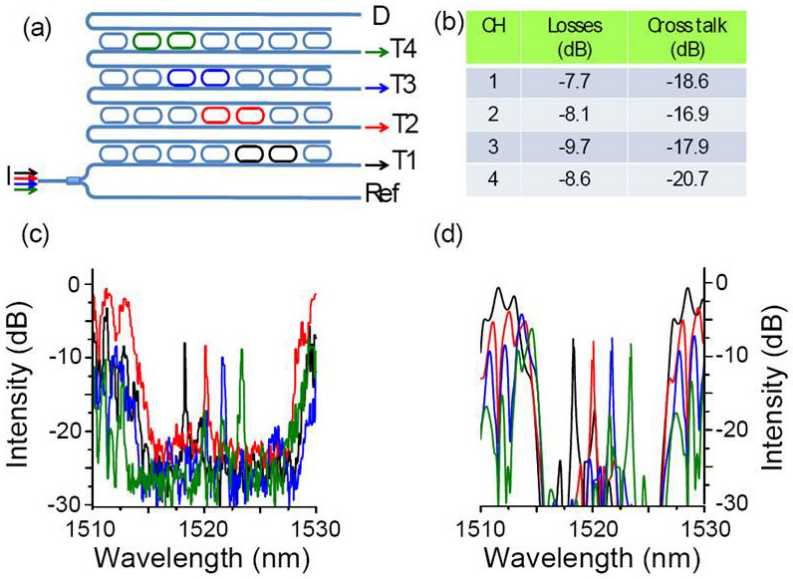

Fig. 5. (a) Sketch of the 1 × 4 mux/demux composed by 4 tapered SCISSOR cascaded via the drop waveguide. Each tapered SCISSOR is designed to have different CRIT resonances. The design parameters are R = 3.250 μm, C = 7 μm, gap = 160 nm, ΔR = 5 nm, L1 = 10.230 μm (T1, black), L2 = 10.220 μm (T2, red), L3 = 10.200 μm (T3, blue), L4 = 10.190 μm (T4, green). (b) Insertion losses and cross talks for each CRIT channel.(c) Experimental transmission spectra for the Through ports: T1 black, T2 red, T3 blue and T4 green; (d) Simulated spectra.

Finally, we demonstrate a 1x4 demultiplexer by using a cascaded sequence of tapered SCISSOR (Fig. 5(a)). Each tapered SCISSOR has the same racetrack sequence but different L. Therefore four different CRIT channels open. Since the four tapered SCISSOR differ solely for a 0.15% variation in L, the wide resonator stop band of each SCISSOR remains largely unaffected and they overlap each others. When the signal wavelength is resonant with the CRIT resonance of a particular tapered SCISSOR, the signal is transmitted out of the demultiplexer (ports T1-T4 in Fig. 5(a)). Otherwise it is dropped as input to the following tapered SCISSOR. Clearly, if the signal wavelength is not resonant with any CRIT resonance it emerges in the output D port. The same structure works as a multiplexer if the input are mirrored.

#174511 - $15.00 USD Received 16 Aug 2012; revised 27 Sep 2012; accepted 27 Sep 2012; published 3 Oct 2012

Figures 5(c) and 5(d) show the experimental as well as the simulated transmissions of each T1-T4 ports of the 1x4 demultiplexer. Within the overlapping stop-bands, four CRIT channels open (linewidth 8 GHz, channel spacing 155 GHz, insertion losses −9 ± 1 dB, cross-talk −19 ± 2 dB). It is important to note that the channel spacing is determined by the value ΔR and is not limited by the width of the resonances. Thus, narrower channel spacing can be easily achieved using either a thermal trimming or larger rings. Despite non negligible value of insertion losses, tapered SCISSOR shows rather low cross talk values. No performance degradation along the sequence is observed which indicates that more tapered SCISSOR can eventually be cascaded. It is remarkable that no trimming of the various racetrack resonances is needed and all tapered SCISSOR channels are aligned. These data confirm the device robustness versus fabrication tolerances. All what has been shown previously also apply to the demultiplexer design: each tapered SCISSOR can route multiple channels, each channel can be individually addressed and reconfigured, and the number of tapered SCISSOR in the cascade is determined by the specific networking needs. Compared to other ring resonator based routers, our implementation has important advantages:

1. it allows a single channel addressing capability based on a true on/off switching mechanism, rather than wavelength shift;
2. it has a very small footprint;
3. despite the rather large number of rings involved, insertion losses are kept at rather small value.

Table 1. Comparison among recent proposed router schemes and our implementation

		Router1 [20]	Router2 [21]	Router3 [22]	This work
Ring Radius	(μm)	50	5	6.735	3.25
Footprint[c]	(mm^2/Ch)	< 0.5	0.015	0.084	0.0053
Channel spacing	(GHz)	100	170	124	155
FWHM[b]	(nm)	0.28	0.08-0.16	0.16	0.1
Extinction Ratio	(dB)	−8	−25	−35	−4
P_{off}[a]	(mW @ −4dB)	22	6.3	0.7	1.5
Crosstalk	(dB)	−12	N.A.	−45	−19
Insertion Losses	(dB)	13	25	N.A.	9

[a] P_{off} is the power needed to switch off by 4dB a single channel.
[b] FWHM is the single resonance linewidth.
[c] Footprint is normalized by the number of routed channels for each scheme.

Table 1 reports a comparison between our design and other recently proposed schemes based on rings resonators. We compare similar though different routers. The column label Router1 refers to a scheme based on Si_3N_4/SiO_2 materials and working in a wavelength at 1310 nm. All the other are based on SOI and work at 1550 nm. Crosstalk of Router2 greatly depends on the channel spacing. Router3 shows great performance in terms of spectral width and tuning efficiency at the expenses of a thermal trimming of the entire router which is quite power consuming (about 16 mW/channel).

The tapered SCISSOR router shows small footprint, low insertion losses and low crosstalk. A proper engineering of the thermal heater could reduce significantly the power needed to close a single channel. In addition, our implementation exploits the properties of tapered SCISSOR to achieve large Q-factor while keeping a very good robustness against fabrication defects. In fact the large stop band that contains all the routed channels is only slightly affected by fabrication defects, thus a reduced amount of power is needed to trim several channels at once.

#174511 - $15.00 USD Received 16 Aug 2012; revised 27 Sep 2012; accepted 27 Sep 2012; published 3 Oct 2012

4. Conclusion

In conclusion, we have demonstrated an innovative tapered SCISSOR design which allows the fabrication of routing and switching devices on the silicon photonics platform for DWDM applications. We show that a proper design of coupled resonators in a resonator sequence yields enhanced properties with respect to single resonator and greatly reduces the effect of the fabrication errors. In particular, the use of coupled resonators enables the achievement of Q-factors much greater than those of the single resonators. SCISSORs operate in the overcoupling regime, thus they keep low insertion losses and high power transfer among add/drop channels. Furthermore, the switching mechanism is a true on/off switch that implies a negligible spectral shift of the resonance and eases the realization of dense wavelength division multiplexing routers. Data transmission up to 3 Gbps (limited by our experimental setup) was experimentally demonstrated, while much faster rate is envisioned. In this work we have demonstrated a single method to induce the coupling among the different resonators in the resonator sequence, other possibilities exist [12].

#174511 - $15.00 USD Received 16 Aug 2012; revised 27 Sep 2012; accepted 27 Sep 2012; published 3 Oct 2012